Extender:

A Case Study for Human-Robot Interaction via

Transfer of Power and Information Signals

H. Kazerooni

Mechanical Engineering Department
University of California at Berkeley
Berkeley, CA 94720 USA
kazerooni@euler.berkeley.edu

ABSTRACT

A human's ability to perform physical tasks is limited by physical strength, not by intelligence. We define "extenders" as a class of robot manipulators worn by humans to augment human mechanical strength, while the wearer's intellect remains the central control system for manipulating the extender. Our research objective is to determine the ground rules for the control of robotic systems worn by humans through the design, construction, and control of several prototype experimental direct-drive/non-direct-drive multi-degree-of-freedom hydraulic/electric extenders. The design of extenders is different from the design of conventional robots because the extender interfaces with the human on a physical level. Two sets of force sensors measure the forces imposed on the extender by the human and by the environment (i.e., the load). The extender's compliances in response to such contact forces were designed by selecting appropriate force compensators. The stability of the system of human, extender, and object being manipulated was analyzed. A mathematical expression for the extender performance was determined to quantify the force augmentation. Experimental studies on the control and performance of the experimental extender were conducted to verify the theoretical predictions.

NOMENCLATURE

All matrices and vectors are nxn and nx1, where n is the number of degrees of freedom for the extender. The Laplace arguments of the transfer functions and the arguments of nonlinear operators are shown in the nomenclature but are dropped in the text.

$E(p)$ a vector, nonlinear operator; representing the load dynamics

$E_0(s)$ a transfer function matrix; representing the linear portion of the load dynamics

f_e a vector; the force imposed on the extender by the load

f_{ext} a vector; any force imposed on the load by external objects other than the extender or the human arm

f_h a vector; the force imposed on the extender by a human arm

f_h^* a vector; the force imposed on the extender by an arm at no-load condition

$G(s)$ a matrix; the closed loop transfer function mapping desired position, p_{des} to extender endpoint position, p

$H(p)$ a vector, nonlinear operator representing human arm dynamics

$H_0(s)$ a transfer function matrix representing the linear portion of the human arm dynamics

$K(s)$ a transfer function matrix representing the stability controller

n the degrees of freedom of the extender

p a vector; the actual position of the extender endpoint

p_{des} a vector; the desired position of the extender endpoint

$R(s)$ a matrix; the performance index

s the Laplace operator (sec^{-1})

$S_e(s)$ a matrix; the sensitivity transfer function mapping load force f_e to extender position, p

$S_h(s)$ a matrix; the sensitivity transfer function mapping human force f_h to extender position, p

u_h a vector; the human muscle force which initiates a maneuver

$\alpha(s)$ a transfer function matrix representing the controller operating on the human force, f_h

$\Delta(p)$ a vector, operator representing the nonlinear dynamics in the human and the load

ω_p frequency range of operation

ε scalar

$\lambda_{Gc}, \lambda_\Delta, \beta_{Gc}, \beta_\Delta, \beta_{in}$: scalar constants

1. INTRODUCTION

This article describes the dynamics and control of a human-integrated material handling system. This material handling equipment is a robotic system worn by humans to increase human mechanical ability, while the human's intellect serves as the central intelligent control system for manipulating the load. These robots are called extenders due to a feature which distinguishes them from autonomous robots: they extend human strength while in physical contact with a human[1]. The human becomes a part of the extender, and "feels" a force that is related to the load carried by the extender.

Figure 1 shows an example of an extender. Some major applications for extenders include loading and unloading of missiles on aircraft; maneuvering of cargo in shipyards, foundries, and mines; or any application which requires precise and complex movement of heavy objects.

The goal of this research is to determine the ground rules for a control system which lets us arbitrarily specify a relationship between the human force and the load force. In a simple case, the force the human feels is equal to a scaled-down version of the load force: for example, for every 100 pounds of load, the human feels 5 pounds while the extender supports 95 pounds. In another example, if the object being manipulated is a pneumatic jackhammer, we may want to both filter and decrease the jackhammer forces: then, the human feels only the low-frequency, scaled-down components of the forces that the extender experiences. Note that force reflection occurs naturally in the extender, so the human arm feels a scaled-down version of the actual forces on the extender without a separate set of actuators.

---

[1] These robots are sometimes referred to as Personnel Amplification Systems (PAS).

Three elements contribute to the dynamics and control of this material handling system: the human operator, an extender to lift the load, and the load being maneuvered. The extender is in physical contact with both the human and the load, but the load and the human have no physical contact with each other. Figure 2 symbolically depicts the communication patterns between the human, extender, and load. With respect to Figure 2, the following statements characterize the fundamental features of the extender system.
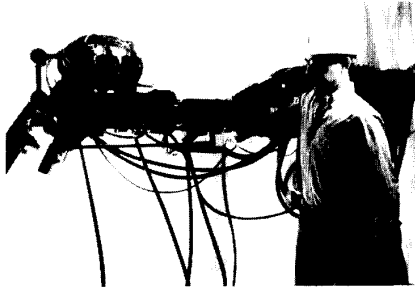

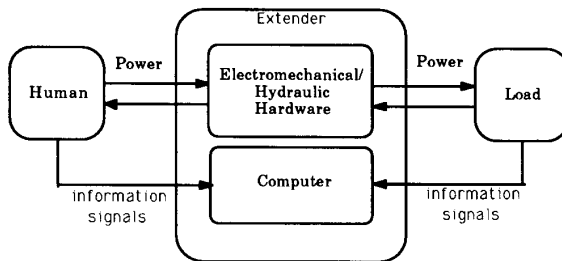*Figure 1: Experimental Six-Degree-of-Freedom Hydraulic Extender.*

Figure 2: The extender motion is a function of the forces from the load and the human, in addition to the command signal from the computer.

1) The extender is a powered machine and consists of: 1) hardware (electromechanical or hydraulic), and 2) a computer for information processing and control.

2) The load position is the same as the extender endpoint position. The human arm position is related kinematically to the extender position.

3) The extender motion is subject to forces from the human and from the load. These forces create two paths for power transfer to the extender: one from the human and one from the load. No other forces from other sources are imposed on the extender.

4) Forces between the human and the extender and forces between the load and the extender are measured and processed to maneuver the extender properly. These measured signals create two paths of information transfer to the extender: one from the human and one from the load. No other external information signals from other sources (such as joysticks, pushbuttons or keyboards) are used to drive the extender.

The fourth characteristic emphasizes the fact that the human does not *drive* the extender via external signals. Instead, the human moves his/her hands naturally when maneuvering an object. Clarification of this natural control is found in the following. If "talking" is defined as a natural method of communication between two people, then we would like to communicate with a computer by talking rather than by using a keyboard. The same is true here: if

"maneuvering the hands" is defined as a natural method of moving loads, then we would like to move a load by maneuvering the hands, rather than by using a keyboard or joystick.

Considering the above, human-machine interaction can be categorized into three types:

1) Human-machine interaction via the transfer of power
   In this category, the machine is not powered and therefore cannot accept information signals (commands) from the human. A hand-operated carjack is an example of this type of machine; to lift a car, one imposes forces whose power is conserved by a transfer of all of that power to the car. This category of human-machine interaction includes screw-drivers, hammers, and all similar unpowered tools which do not accept information signals but interact with humans or objects through power transfer.

2) Human-machine interaction via the transfer of information
   In this category, the machine is powered and therefore can accept command signals. An electric can opener is a machine which accepts command signals. No power is transferred between the can opener and the human; the machine function depends only on the command signals from the human.

3) Human-machine interaction via the transfer of both power and information signals
   In this category, the machine is powered and therefore can accept command signals from the human. In addition, the structure of the machine is such that it also accepts power from the human. Extenders fall into this category. Their motions are the result not only of the information signals (commands), but also of the interaction force with the human [14].

This paper focuses on the dynamics and control of machines belonging to the third category of interaction involving the transfer of both information signals and power. The information signals sent to the extender computer must be compatible with the power transfer to the extender hardware. This paper presents this compatibility in terms of closed-loop stability. We first model the system elements shown in Figure 2 in the sense of both power and information signals. We then address the dynamic performance that one may want in an extender. This leads us to the control techniques for and the stability conditions of such machines. We then discuss a series of experiments we conducted to verify the dynamic performance of an experimental two-degree-of-freedom electric extender.

The objective of this research effort is to determine the rules for the control of robotic systems worn by humans through the design, construction, and control of a prototype experimental extender. Section 2 reviews the history of devices similar to the extender. Section 3 gives an overall view of the systems dynamic behavior. Section 4 and 5 discuss the control system architecture. Section 6 presents experimental results pertaining to the stability and performance of this experimental extender. Section 7 offers conclusions drawn from this effort.

2. HISTORY

The concept of a device which could increase the strength of a human operator using a master-slave system has existed since the early 1960s. The concept was originally given the name "man-amplifier". The man-amplifier was defined as a type of manipulator which greatly increases the strength of a human operator, while maintaining the human's supervisory control of the manipulator.

In the early 1960s, the Department of Defense was interested in developing a powered " suit of armor" to augment the lifting and carrying capabilities of soldiers. The original intent was to develop a system which would allow the human operator to walk and manipulate very heavy objects. Research was done for the Air Force in 1962 at the Cornell Aeronautical Laboratory to determine the feasibility of developing a master-slave system to accomplish this task. This study found that duplicating all human motions would not be practical, and that further experimentation would be

required to determine which motions were necessary. It was also determined that the most difficult problems in designing the man-amplifier were in the areas of servo, sensor and mechanical design [4]. Further work at the Cornell Aeronautical Laboratory determined that an exoskeleton having far fewer degrees of freedom than the human operator would be sufficient to carry out most desired tasks. In 1964 Cornell developed a preliminary arm and shoulder design. This design demonstrated that the amplifying ability of the manipulator was limited by the physical size of the hydraulic actuators required to amplify the human operator's strength [22, 23, 24].

From 1966 to 1971 General Electric completed work on the man-amplifier concept through prototype development and testing. This man-amplifier, known as the Hardiman, was a system of two overlapping exoskeletons worn by the human operator and was designed as a master-slave system. The master was the inner exoskeleton, which moved due to the motions of the operator. The slave was the hydraulically-actuated outer exoskeleton, which followed the motions of the master. Thus, the slave exoskeleton also followed the motions of the human operator [9, 10, 11, 20].

It is important to note that previous systems (described above) operated based on the master-slave concept, rather than on the direct physical contact between human and manipulator inherent in the extender concept. Unlike the Hardiman and other man-amplifiers, the extender is not a master-slave system (i.e. it does not consist of two overlapping exoskeletons.) There is no joystick or other device for information transfer. Instead, the human operator's commands to the extender are taken directly from the interaction force between the human and the extender. This interaction force also helps the extender manipulate objects physically. In other words, information signals and power transfer simultaneously between the human and the extender. The load forces naturally oppose the extender motion. The controller developed for the extender translates this interaction force signal into a motion command for the extender. This allows the human to initiate tracking commands to the extender in a very direct way. The concept of transfer of power and information signals is also valid for the load and extender. The load forces are measured directly from the interface between the load and the extender and processed by the controller to develop electronic compliancy [13, 16, 17, and 18] in response to load forces. In other words, information signals and power transfer simultaneously between the load and the extender [15].

Several prototype experimental extenders were designed and built by H. Kazerooni o help clarify the design and control issues for various payloads and maneuvering speeds.

Prototype 1: One-Degree-of-Freedom Extender [14]

To study the feasibility of human force amplification via hydraulic actuators, a one-degree-of-freedom extender was built (Figure 3). This experimental extender consists of an inner tube and an outer tube. The human arm, wrapped in a cylinder of rubber for a snug fit, is located in the inner tube. A rotary hydraulic actuator, mounted on a solid platform, powers the outer tube of the extender. A piezoelectric load cell, placed between the two tubes, measures the interaction force between the extender and the human arm. Another piezoelectric load cell, placed between the outer tube and the load, measures the interaction force between the extender and the load. Other sensing devices include a tachometer and encoder (with corresponding counter) to measure the angular speed and orientation. A microcomputer is used for data acquisition and control. We developed a stabilizing control algorithm which creates any arbitrary force amplification and filtering. This study led to understanding the nature of extender instability resulting from human-machine interaction.

Prototype 2: Two-Degree-of-Freedom Direct-Drive Electric Extender

To develop and test nonlinear control algorithms, a direct-drive, electrically-powered extender was built (Figure 4). The direct connection of the motors to the links (without any transmission systems) produces highly nonlinear behavior in the extender [18]. This extender has two degrees of freedom corresponding to a shoulder and an elbow. Two motors are located at the same height

as the average human shoulder. Force sensors are located at the human-extender and extender-load interfaces. A third degree of freedom may be added: either rotation about a vertical axis or roll about a horizontal fore-aft axis.

Figure 3: The first experiment: a one-degree-of-freedom hydraulic extender to observe the effect of hydraulic actuation on extender performance.
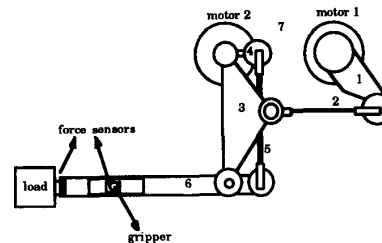

Figure 4: The second experiment: a two-degree-of-freedom direct-drive experimental extender to verify the feasibility of using direct-drive actuators for high-speed maneuvers of loads weighing less than 50 lb.

Prototype 3: Two-Degree-of-Freedom Non-Direct-Drive Electric Extender [15]

Figure 5 shows the experimental planar two-degree-of-freedom non-direct-drive extender used to study the extender performance in non-direct-drive systems. The operator grasps a handle mounted on a piezoelectric force sensor in contact with a table; this sensor measures the human's force on the table along the x and y directions. A mass is suspended below the table from another piezoelectric force sensor; this sensor measures the force imposed on the extender (i.e., table) by the load in the plane of motion. Other sensing devices include a tachometer and an encoder (with a corresponding counter) to measure the speed and position of the table. The study which used this experimental extender showed that non-direct-drive extenders have a large stability range, but cannot keep up with the wide bandwidth motion of the human. In this study we arrived at the trade-offs between stability and the size of the extender impedance which are caused by extender non-backdrivability. A large impedance in the extender due to its non-

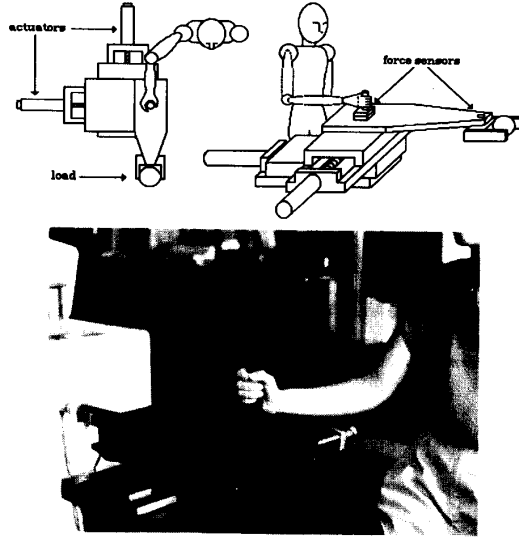backdrivability reduces the effect of the human impedance and results in greater stability.

Figure 5: The third experiment: a two-degree-of-freedom non-direct-drive experimental extender to verify the feasibility of using non-direct-drive actuators to maneuver loads weighing less than 200 lb.

Prototype 4: Extender Walking Machine

Figure 6 shows one of our experimental walking machines which helped us learn how to control a machine that must stand on its own. This experimental machine has two links which are powered relative to each other by a DC motor at joint 2. Joint 1 at ground level is not powered: a motor at joint 1 would require an prohibitively large and lengthy foot similar to a snow ski. We have developed an actuation mechanism and a control technique which stabilize the mass on top of the second link without the use of any gyro. This is a first and very fundamental issue in the design and control of walking machines for the extender.

Figure 6: An experimental walking machine consisting of two links. Only joint 2 is powered. Joint 1 is not powered and sits on the ground. The goal of our research has been to stabilize this machine with one actuator only. The actuator at Joint 2 must be controlled in such a way that the center of mass of the entire system passes through Joint 1.

3. MODELING

This section models the dynamic behaviors of the extender, the human arm and the load being maneuvered; these models are combined in Figure 2. It is assumed that the extender primarily has a closed-loop position controller, which is called the *primary stabilizing controller*. The resulting closed-loop system is called the *primary closed-loop system*. The design of the primary stabilizing controller must consider the following three issues.

1) Exact dynamic models for the extender are difficult to produce because of uncertainties in the dynamics of the extender actuators, transmissions and structure. These uncertainties become a major barrier to the achievement of the desired extender performance, especially when human dynamics are coupled with the extender dynamics in actual machine maneuvers. The extender's primary stabilizing controller minimizes the uncertainties in the extender dynamics and creates a more definite and linear dynamic model for the extender. Therefore, it is assumed that the dynamics of the extender are linearized by the primary stabilizing controller over a range of operation. This linear model may then be used to design other controllers that operate on forces f_h (i.e., the human force) and f_e (i.e., the load force). For the experimental extender employed in this research effort, the computed-torque method along with a PD controller [1, 2] is used as the primary stabilizing controller to create a more definite and linear dynamics for the extender.

2) Extender stability must be guaranteed when the human is not maneuvering the extender. This is a very important safety feature: when the human separates his/her hand from the extender in emergency situations, the primary stabilizing controller must hold the extender stationary at the configuration at which the human arm separated from the extender.

3) The design of the primary stabilizing controller must let the designer deal with the effect of the extender uncertainties without concern for the dynamics of the human operator. The human arm dynamics, unlike the extender dynamics, change significantly with each human and also within one person over time [12, 25]. Considering the control difficulties arising from the human and load nonlinear dynamics, it is a practical matter to make every effort in developing a linear dynamic behavior for the extender.

The selection of the primary stabilizing controller is not discussed here; a variety of controllers may be used to stabilize the extender in the presence of uncertainties and nonlinearities. These controllers result in uncoupled and linearized closed-loop behavior for the extender within a certain frequency range [28].

Regardless of the type of primary stabilizing controller, the extender position, p, results from two inputs: 1) the desired position command, p_{des}, and 2) the forces imposed on the extender. The transfer function matrix G represents the primary closed-loop position system which maps p_{des} to the extender position, p. Two forces are imposed on the extender: f_h is imposed by the human, and f_e is imposed by the load. S_h, an extender sensitivity transfer function, maps the human force, f_h, onto the extender position, p. Similarly, S_e, an extender sensitivity transfer function, maps the load force, f_e, onto the extender position, p. If the primary stabilizing controller is designed so that S_h and S_e are small, the extender has only a small response to the imposed forces f_h and f_e. A high-gain controller in the primary stabilizing controller results in small S_h and S_e and consequently a small extender response to f_h and f_e. Using G, S_e and S_h, equation 1 represents the dynamic behavior of the extender.

$$p = G \ p_{des} + S_h \ f_h + S_e \ f_e \tag{1}$$

The middle part of the block diagram in Figure 7 represents the extender model (i.e., equation 1) interacting with the human and the load. The upper left part of the block diagram represents the

human dynamics. The human arm's force on the extender, f_h, is a function of both the human muscle forces, u_h, and the position of the extender, p. Thus, the extender's motion may be considered to be a position disturbance occurring on the force-controlled human arm. If the extender is stationary (i.e., p = 0), then the force imposed on the extender is solely a function of the human muscle force command produced by the central nervous system. Conversely, if the extender is in motion and u_h = 0, then the force imposed on the extender is solely a function of the human arm impedance, H(p). H is a nonlinear operator representing the human arm impedance as a function of the human arm configuration; H is determined primarily by the physical properties of the human arm [5, 19, 27]. Based on the above, equation 2 represents a dynamic model of the human arm.

$$f_h = u_h - H(p) \qquad (2)$$

The specific form of u_h is not known other than it results from human muscle force on the extender. A simple study of how the central nervous system generates the desired force command u_h is given in [6, 8]. The experimental procedure to measure H from various subjects is given in Section 6.

It is assumed that the extender is maneuvering a load. The load force impedes the extender motion. The extender controller translates the two measured interaction forces (i.e., the human forces and load forces) into a motion command for the extender to create a desired relationship between the human forces and the load forces. E is a nonlinear operator representing the load dynamics. f_{ext} is the equivalent of all the external forces imposed on the load which do not depend on p and other system variables. Equation 3 provides a general expression for the force imposed on the extender, f_e, as a function of p.

$$f_e = - E(p) + f_{ext} \qquad (3)$$

In the example of accelerating a point mass m along a horizontal line, the load force, f_e, can be characterized by $f_e = ms^2 p$. In this case $E = ms^2$ and $f_{ext} = 0$ where p is the mass position and s is the Laplace operator. If the load is large and cannot be represented by a point mass, then E can be calculated using Lagrangian formulation.
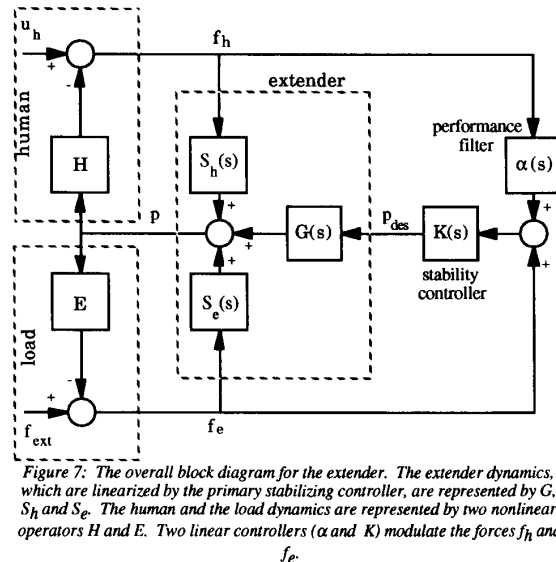

Figure 7: The overall block diagram for the extender. The extender dynamics, which are linearized by the primary stabilizing controller, are represented by G, S_h and S_e. The human and the load dynamics are represented by two nonlinear operators H and E. Two linear controllers (α and K) modulate the forces f_h and f_e.

The diagram of Figure 7 includes two linear controllers, α(s) and K(s), which modulate the forces f_h and f_e. α and K (which are implemented on a computer) must be designed to produce a desired

performance in the extender system; this is described in the next section. As the Figure 7 block diagram shows, the performance filter α lets designers choose the appropriate performance for the extender, and the stability filter K (which operates on both f_h and f_e) guarantees the system stability when the extender is used by people with various arm impedances (strengths).

4. CONTROL

To understand the role of controllers α and K, assume for a moment that neither controller is included in the system. If the commanded position, p_{des}, the human muscle forces, u_h, and the external forces, f_{ext}, all equal zero, then the extender position, p, equals zero, and no motion is transmitted to the load. This is the case when the human is holding the extender without intending to maneuver it. If the human decides to initiate a maneuver, then u_h takes on a nonzero value, and an extender motion develops from f_h. The resulting motion is small if S_h is small. In other words, the human may not have enough strength to overcome the extender's primary closed-loop controller.

To increase the human's effective strength, the extender's effective sensitivity to f_h must be increased by measuring the human force, f_h, and passing it through the controllers α and K. Figure 7 shows that GKα, parallel with S_h, increases the effective sensitivity of the extender to f_h. To retain a sense of the load in the extender operation, the load force, f_e, is also measured and passed through K. This produces the loop GK, parallel with S_e, which increases the effective sensitivity of the extender to f_e. The output of K is applied to the extender as a desired position command, p_{des}. K and α must be chosen to ensure the stability and performance of the closed-loop extender system. The proper choice of K and α achieves a desired ratio of human force to load force, and guarantees the closed-loop stability of Figure 7[2]. Note that both the human force, f_h, and load force, f_e, are measured for feedback to the extender: the measure of f_h (after passing through α and K) will move the extender, while f_e (after passing through K) will impede the extender motion.

Next, the following question is addressed: how should the extender perform in a particular maneuver? In specifying the extender's performance, the designers decree the important criteria which must be met for the successful completion of a maneuver. Also in the performance specification, the designers describe the extender behavior they find desirable if stability can be maintained. Performance goals and stability requirements do conflict. As is clarified in the next section, the designers must balance this trade-off to develop an extender that both performs well and is guaranteed to be stable.

The following example illustrates a simple specification for the extender performance. The human uses the extender to maneuver a free mass in space. A reasonable performance specification for this example would state the level of amplification of the human force which is applied to the free mass. If the force amplification is large, a small force applied by the human results in a large force being applied to the free mass. If the amplification is small, a small force applied by the human results in a small force being applied to the free mass. Consequently, if the amplification is large, the human "feels" only a small percentage of the interaction force with the free mass. Most importantly, the human still retains a sensation of the dynamic characteristics of the free mass, yet the load essentially "feels" lighter.

---

2   Another way of interpreting K and a is as follows. K is a linear controller that servos the difference between (f_e) and (αf_h) to zero.

With these heuristic ideas of system performance, the extender performance is captured in equation 4 where $f_h{}^*$ is the human force applied to maneuver the extender when no load is present. R is the *performance matrix*, and $[0,\omega_p]$ is the frequency range of the human arm motion.

$$(f_h - f_h{}^*) = -R\, f_e \qquad \text{for all } \omega \in [0,\omega_p] \qquad (4)$$

Equality 4 guarantees that $(f_h - f_h{}^*)$, the portion of the human force that is actually applied to maneuver the load, is proportional to the load force, f_e. The performance matrix R is an nxn linear transfer function matrix. Suppose R is chosen as a diagonal matrix with all members having magnitudes smaller than unity over some bounded frequency range, $[0, \omega_p]$. Then the human force is smaller than the load force by a factor of R. Suppose R is chosen as a diagonal matrix with all members having magnitudes greater than unity. Then the human force is larger than the load force by a factor of R. In a more complex example, the transfer function matrix R may be selected to represent linear passive dynamic systems (i.e., combinations of dampers, springs and masses). The frequency range $[0,\omega_p]$, implies the desired frequency range in which the designers wish to operate the extender (i.e. human motion). Specifying ω_p allows the designers to achieve equality 4 only for a bounded frequency range; there is no need to achieve equation 4 for an infinite bandwidth. Establishing the set of performance specifications described by equation 4 gives designers a chance to express what they wish to have happen during a maneuver. Note that equation 4 does not imply any choice of control technique for the extender. We have not even said how one might achieve the above performance specification. Equation 4 only allows designers to translate their objectives into a form that is meaningful from the standpoint of control theory.

By inspecting Figure 7, the extender position is written as a function of f_h and f_e.

$$p = (G K \alpha + S_h)\, f_h + (G K + S_e)\, f_e \qquad (5)$$

Now suppose that the human maneuvers the extender through the same trajectory indicated by p in equation 5 except without any load. The no-load human force, $f_h{}^*$, is then obtained by inspection of Figure 7 where $E = 0$ and $f_{ext} = 0$:

$$p = (G K \alpha + S_h)\, f_h{}^* \qquad (6)$$

Equating the trajectories from equations 5 and 6 results in equation 7.

$$(f_h - f_h{}^*) = -(G K \alpha + S_h)^{-1} (G K + S_e)\, f_e \qquad (7)$$

Comparing equations 4 and 7 shows that to guarantee the performance represented by R in equation 4, inequality 8 must be satisfied.

$$\sigma_{max} [(G K \alpha + S_h)^{-1} (GK + S_e) - R] < \varepsilon$$
$$\text{for all } \omega \in [0, \omega_p] \qquad (8)$$

σ_{max} represents the maximum singular value. ε represents a small positive number chosen by the designer to denote the degree of precision required for the specified performance within the frequencies $[0, \omega_p]$. A small value for ε (e.g., 0.01) indicates a close proximity of the actual system performance to the specified performance R (e.g., within a 1% error). Note that the human and load dynamics, H and E, are absent from inequality 8. Thus, achievement of the specified performance R depends only on the extender dynamic behavior (G, S_e, S_h) and on the controllers (K,

α), and not on the particular human operator and load. However the stability of the closed-loop system in Figure 7 which depends on E and H must be guaranteed.

Satisfaction of inequality 8 guarantees that the performance defined by equation 4 is achieved with precision ε. Therefore, the goal is to select K and α so condition 8 is satisfied. Assuming that R is selected so R^{-1} always exists, α is chosen to be equal to R^{-1}. (This unexpected choice for α results from investigations of several design methods). Substituting R^{-1} for α in inequality 8 shows that any K which satisfies inequality 9 also satisfies inequality 8.

$$\sigma_{max} (GK) > \frac{\sigma_{max} (S_e - S_h\, R)\; \sigma_{max}\, (R)}{\varepsilon}$$
$$\text{for all } \omega \in [0, \omega_p] \qquad (9)$$

Inequality 9 suggests that, since ε is a small number, the designer must choose K to be a transfer function matrix with large magnitude to satisfy inequality 9 for frequencies $\omega \in [0, \omega_p]$ and for a given ε, R, S_h and S_e. The smaller ε is chosen to be, the larger K must be to achieve the desired performance. K may not be arbitrarily very large: the choice of K must also guarantee the closed-loop stability of the system shown in Figure 7, as discussed in the next section.

5. STABILITY

It has been shown that, to achieve the system performance indicated by R, α must be equal to R^{-1} and K must be a large transfer function matrix satisfying inequality 9. However, the designers must realize that the closed-loop system of Figure 7 must remain stable for these choices of α and K. The selection of K is particularly important since H and E generally contain nonlinear dynamic components. For example, the human arm impedance H changes from person to person and also within one person over time. The load dynamics E is also a nonlinear element as discussed earlier. Compared to the human arm and load dynamics, the extender dynamics (G, S_e, S_h) are generally well-defined due to the primary stabilizing controller. Consequently, this analysis focuses on designing a stabilizing controller K in the presence of all bounded variations of the nonlinear operators H and E with G, S_e and S_h being known and linear dynamics. The following questions illuminate our approach to the design of K.

In designing K, is it possible to work with a human and a load with linear dynamics (represented by H_O and E_O) instead of the nonlinear dynamics represented by operators H and E? If the answer is yes, then what properties should H_O and E_O have so that the designed K both satisfies inequality 9 and stabilizes the Figure 7 system in the presence of a family of nonlinear operators H and E?

The block diagram of Figure 7 is transformed into the block diagram of Figure 8 in order to group the nonlinear operators, H and E, into one block on the diagram.
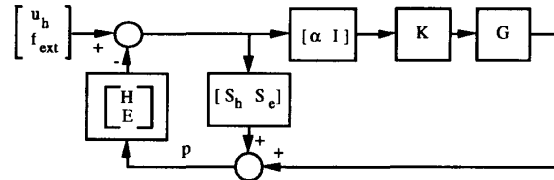

Figure 8: Simplified block diagram of Figure 7. I is a unity matrix.

S_h and S_e represent the sensitivities of the extender position to the human and load forces. G, S_h and S_e depend on the nature of the extender's primary stabilizing controller. If a primary stabilizing controller with a large position loop-gain or integral control is chosen to insure small steady state errors, then S_h and S_e are extremely small compared to G, approaching zero at steady-state. Prototype extender designs have produced sensitivities on the order of 10^3 to 10^6 times smaller than G [15]. If the extender actuators are non-backdrivable, as in systems with geared large transmission ratios, then S_h and S_e are zero regardless of how carefully the extender's primary stabilizing controller is chosen. Since S_h and S_e are typically much smaller than G, their effect on the overall system dynamics is negligible. Therefore S_h and S_e are disregarded in the following stability analysis. Figure 9 presents the resulting simplified stability diagram. Note that the stacked nature of the input signal, the human and load dynamics in Figure 9 are now reduced to single entities where (αH+E) is a nonlinear operator, and K and G are transfer function matrices.
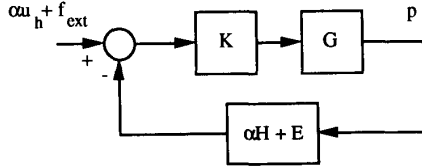
Figure 9: In systems with very small sensitivity transfer functions, S_e and S_h are much smaller than G and their effect on the overall system dynamics is negligible.

If H_0 and E_0 are assumed to represent a particular set of linear human and load dynamics, equation 10 represents the general form of H and E where Δ is the stable nonlinear part of the dynamics. In cases where the nonlinear dynamics may not be directly separated from the linear dynamics, an estimate of H_0 and E_0 must be formed from experiments such as those in Section 6.

$$\alpha H(p) + E(p) = [\alpha\, H_0 + E_0]\, p + \Delta(p) \qquad (10)$$

Note that $[\alpha\, H_0 + E_0]$ is a transfer function matrix operating on p. The block diagram of Figure 9 can be transformed into the block diagram of Figure 10 which separates the nonlinear term Δ from the linear terms $[\alpha H_0 + E_0]$.
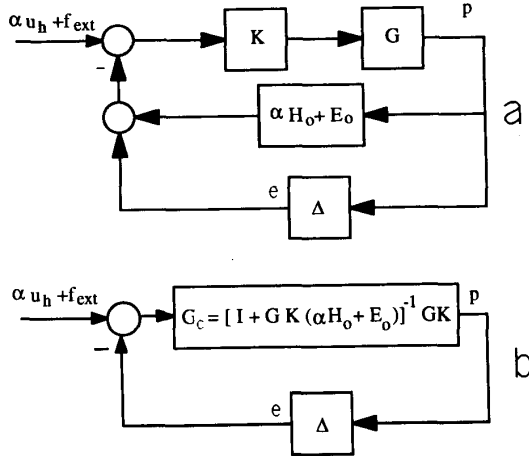

Figure 10: Δ is the stable nonlinear operator representing the nonlinear human and load dynamics.

With respect to Figure 10, the design of K is approached as follows.

A stabilizing controller K must be designed for a set of linear H_0 and E_0 so that the closed-loop system of Figure 10 remains stable and inequality 9 (indicating the performance) is satisfied[3]. This controller must guarantee enough stability robustness for all bounded values of H and E. Therefore the goal is to find a particular class of H_0 and E_0 and a stabilizing controller K that together yield the largest stability robustness for a given largest Δ. Equation 11 represents the forward loop in Figure 10b.

$$G_c = [\, I + GK(\alpha\, H_0 + E_0)\,]^{-1}\, GK \qquad (11)$$

The stability of each element in Figure 10b is described by inequalities 12, 13 and 14:

$$\|\,\alpha\, u_h + f_{ext}\,\|_\infty \le \beta_{in} < \infty \quad \text{"input is } L_\infty \text{ bounded"} \qquad (12)$$

$$\|\, e\, \|_\infty \le \lambda_\Delta\, \|\, p\, \|_\infty + \beta_\Delta \quad \text{"}\Delta \text{ is } L_\infty \text{ stable"} \qquad (13)$$

$$\|\, p\, \|_\infty \le \lambda_{Gc}\, \|\, e\, \|_\infty + \beta_{Gc} \quad \text{"}G_c \text{ is } L_\infty \text{ stable"} \qquad (14)$$

λ and β are finite positive constants that indicate L_∞ stable mappings. The closed-loop system of Figure 10 is L_∞ stable if the norm of the output p is bounded. According to the Small Gain Theorem [7], this is guaranteed if inequality 15 is satisfied[4].

$$\lambda_{Gc}\, \lambda_\Delta < 1 \qquad (15)$$

The human arm impedance H changes from person to person and also within one person over time. This leads to large variations for λ_Δ. To obtain an intuitive feel for the stability condition in inequality 15, evaluation of inequality 15 within the the operating range of the extender system is useful. If K is designed as a very large transfer function in order to guarantee system performance (as prescribed by inequality 9), then equation 11, within the controller bandwidth, may be approximated by:

$$G_c \approx [\alpha\, H_0 + E_0]^{-1} \qquad \text{for all } \omega \in [0,\omega_p] \qquad (16)$$

One must choose the largest load that an extender can manipulate to be E_0, the strongest human impedance to be H_0, and the greatest force amplification as a performance specification to be α_{max}. Then, $[\alpha_{max}\, H_0 + E_0]$ will be larger, and G_c and consequently λ_{Gc} will be smaller. If λ_{Gc} is smaller, then, according to inequality 15, λ_Δ takes on larger values. In other words, if the largest values of α_{max}, H_0 and E_0 are used to design a stabilizing K (i.e., one that guarantees inequality 9), then the closed-loop system will remain stable in the presence of the large variations of human and load dynamics represented by a large λ_Δ. See References 13 and 18 for similar studies on stability of robotic compliant maneuvers.

Inequality 9 also teaches that a large K is needed to guarantee achievement of the system performance. Inspection of Figure 9 shows that choosing a large $[\alpha_{max}H_0+E_0]$ for stability robustness (as discussed above) restricts the designer's choices for a large K.

---

[3] Note that the performance as defined by inequality 9 is independent of H_0 and E_0.

[4] Since G_c, by definition is linear and L_∞-stable, λ_{Gc} is defined as the A-norm of the impulse response of G_c, and β_{Gc} equals zero. See Reference [13] for linear analysis on constrained robotic maneuvers.

This is true because large values for both K and $[\alpha_{max} H_0 + E_0]$ may cause a large loop gain and consequently an unstable system. Therefore, although choosing a large value for $[\alpha_{max} H_0 + E_0]$ leads to stability robustness, it may prohibit the designer's choosing a large K to satisfy the performance specification in inequality 9. Thus, the better understood the load and human dynamics are, the smaller λ_A will be; this leaves more room to increase K and gain more precision in achieving the desired performance as stated by inequality 9 [5].

6. EXPERIMENTAL ANALYSIS

Extender Dynamics

The prototype six-degree-of-freedom hydraulic extender (Figure 1) is used to verify experimentally the theoretical predictions of the extender's stability and performance. The primary functions of the extender shown in Figure 1 are grasping and manipulating heavy objects. The prototype hydraulic extender's hand linkage performs the grasping function while the arm mechanism executes the load manipulations. The arm mechanism (shown in Figure 11) consists of a forearm and an upper arm and has three degrees of freedom. The rotational axes of the extender arm are designed to coincide with those of the human arm joints. Both the upper arm and the forearm are planar four-bar linkages. The upper arm is driven by actuator A2, while the forearm is driven by actuator A3. Both actuators 2 and 3 are located on a bracket which rotates in response to the rotation of actuator A1. Actuator A1 is anchored to a base which is attached to the ground so the extender is not mobile. The arm uses four-bar linkages because: 1) the reaction torque of A2 does not act directly on A3, and vice versa, 2) the weight of one motor is not a load on the other, and 3) both actuators may be placed outside of the human viewing area. Figure 11 also shows a three-direction piezoelectric force sensor that measures the first three components of human force, f_h.

The extender hand mechanism is shown in Figure 12; it has three degrees of freedom. The need to minimize operator fatigue requires that the extender hand be easily integrated with human hand postures. Actuator A5 drives the axis of wrist flexion and extension. For tasks that require secure grasping, humans apply opposing forces around the object. Opposing forces in the extender hand are created by motion of the thumb relative to the wrist via actuator 6. A5 and A6 are both located on a bracket connected to actuator A4 which twists the whole hand mechanism. The human hand is located in a glove which has force sensors mounted at the interfaces between the hand and the glove for measuring the human force, f_h, in six directions. A thin elastic material is used at these contact points for the comfort of the human hand. The human operator can adjust the tightness of this glove simply by moving his/her elbow position horizontally. Several force sensors, not shown in the figure, are also mounted at the gripper to measure the load force, f_e, in six directions. The materials and the dimensions of the extender components are chosen to preserve the structural-dynamic integrity of the extender. Each link is machined as one solid piece rather than as an assembly of smaller parts. The links are made of high strength 7075 aluminum alloy to reduce the weight of the extender[6].

The extender's primary closed-loop controller measures angular position using encoders. The extender linear model has been resulted because of use of a computed torque method for cancellation of the extender gravity and coriolis forces and a PD controller for stabilization and robustness. (For brevity, the selection of the primary stabilizing compensator (i.e., computer torque method and PD controller) is not discussed here. See Reference [2] for a detailed description of such a control method.) Employing this primary controller, the extender closed-loop

dynamics in the Cartesian coordinate frame in all directions can be described by equation 17. This equation has been verified experimentally and its magnitude is shown in Figure 13 within a bounded frequency range. The 30 rad/sec bandwidth in the plot implies that the extender does not respond to frequencies after 30 rad/sec (about 5 Hertz).
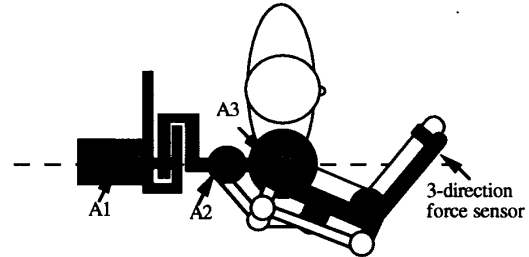

Figure 11: The extender arm has three degrees of freedom. The upper arm is driven by actuator A2, while the forearm is driven by actuator A3. Both actuators 2 and 3 are located on a bracket which rotates in response to the rotation of actuator A1.
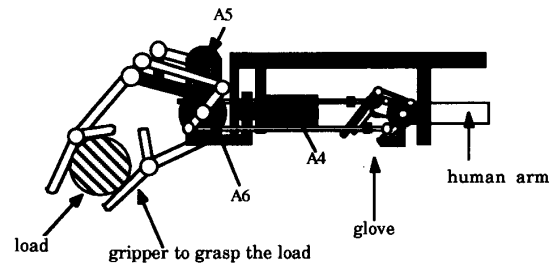

Figure 12: The extender hand has three degrees of freedom. Actuator A4 twists the whole arm while actuators A5 drives the axis of wrist felxion and extension. Actuator A6 opens and closes the gripper.

$$G(s) = \left(\frac{1.565}{\frac{s^2}{3158} + \frac{s}{18.28} + 1.565} \right) \text{ ft/ft} \qquad (17)$$

Note that we have two concerns in achieving the bandwidth of the primary stabilizing controller: 1) human arm frequency range of operation, and 2) extender unmodeled dynamics frequency range. Note that the stability robustness to high frequency unmodeled dynamics in the extender requires small gain for the primary stabilizing controller at high frequencies while tracking the human arm motion requires large gain for the primary stabilizing controller within the frequency range of human arm maneuvers. We will learn in the next section that the normal human arm maneuvers contain frequency components of about up to 3 Hertz. Therefore the primary stabilizing controller loop has been shaped to cross over at frequencies less than the frequency range of extender unmodeled dynamics. This resulted in 5 Hertz bandwidth for the extender which is sufficient for various normal maneuvers. To achieve a wide bandwidth for the extender, designers should have a good model of the extender at high frequencies and consequently, a weak set of stability robustness specifications at high frequencies. It will be shown later that the 5 Hertz bandwidth will become the major impediment in achieving the desired force amplification at high frequency maneuvers.

The primary stabilizing controller also develops very small sensitivity for the extender. Equations 18 and 19 show the extender sensitivity in response to a human force and the load force in actuator A1 only. The small DC gains given by equations 18 and 19 imply strong non-backdrivability; this has resulted from the large supply pressure and large PD gains for the primary stabilizing controller. Since the sensitivity of all actuators are within the range given by equations 18 and 19, the rest of the experimental analysis

---

[5] As Mick Jagger wrote: "you can't always get what you want".

[6] This article is dedicated to the dynamics and control of the extender as it interacts with the human and the load. The details kinematic, dynamic and structural analysis of the extender is not being described here in this article.

assumes $S_h = 0$ and $S_e = 0$. See Reference [21] for dynamics of the servovalves and hydraulic rotary actuators.

$$S_h(s) = 85.0 \times 10^{-6} \frac{\frac{s}{18.6} + 1}{\left(\frac{s^2}{3158} + \frac{s}{18.28} + 1.565 \right)} \quad \text{rad/lbf} \quad (18)$$

$$S_e(s) = 151 \times 10^{-6} \frac{\frac{s}{18.6} + 1}{\left(\frac{s^2}{3158} + \frac{s}{18.28} + 1.565 \right)} \quad \text{rad/lbf} \quad (19)$$
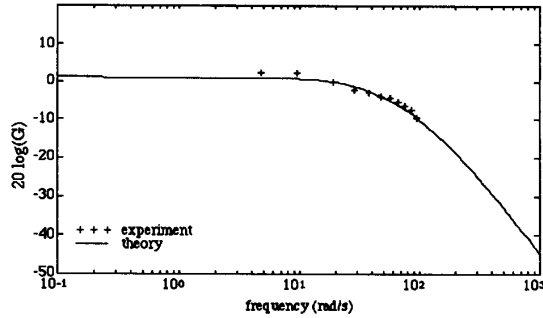

Figure 13: Theoretical and experimental frequency response of the primary closed loop system from input command to extender position.

Human Arm Dynamics

The human arm dynamics do not affect performance (defined by inequality 9) but do play a major role in extender stability. Several experiments were conducted to measure the human arm impedance represented by H. Then the largest of these impedances was chosen to be H_0 in the stability analysis. In the experiments, the subject grasped a handle on the extender. The extender was commanded to oscillate via sinusoidal functions. (See Reference [3] for more detailed information about the nature of such experiments.) At each oscillation frequency, the human operator tried to move his/her hand to follow the extender so that zero contact force would be maintained between the hand and the extender. The human arm, when trying to maintain zero contact forces, cannot keep up with the high-frequency motion of the extender. Thus, large contact forces and consequently a large H are expected at high frequencies. Since this force is equal to the product of the extender acceleration and human arm inertia (Newton's Second Law), at least a second-order transfer function is expected for H at high frequencies. At low frequencies (in particular at DC), the operator can follow the extender motion comfortably, and can establish almost constant contact forces between the hand and the extender. Thus, small contact forces at all extender positions and consequently a constant transfer function for H are expected at low frequencies.

Figures 14 and 15 show the experimental values and the fitted transfer functions for two different experiments. In the first set of experiments (Figure 14), the subject holds the extender handle loosely. In the second set of experiments (Figure 15), the subject holds the extender very tightly. At low frequencies, the human arm impedance is smaller when the subject holds the handle loosely than when the subject holds the handle very tightly. Also note that both plots show a crossover at about 20 rad/sec; this is in the neighborhood of frequencies at which the central nervous system can no longer keep up with the extender motion. The largest impedance, that of Figure 15, is chosen for use in the stability analysis.

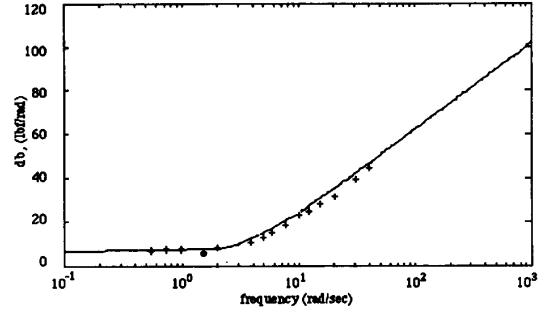$$H_0 = 12.1 \left(\frac{s^2}{43.69} + \frac{s}{5.08} + 1 \right) \quad \text{lbf/ft} \quad (20)$$

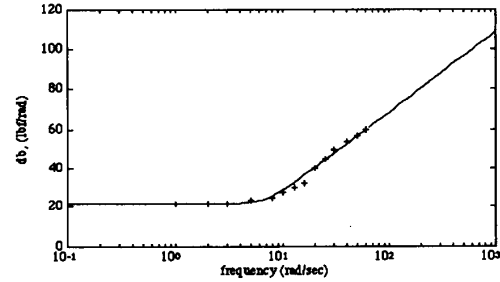Figure 14: The experimental and theoretical plot of H; the human operator holds the extender loosely.

Figure 15: The experimental and theoretical plot of H; the human operator is holding the extender tightly.

Performance

The experimental extender is capable of lifting of objects up to 500 lb when the supply pressure is set at 3000 psi. Since the high frequency maneuvers of 500 lb load is rather unsafe, the experimental analysis on the extender dynamic behavior was carried out at low level of force amplification. In order to observe the system dynamics within the extender bandwidth, in particular the extender instability, the supply pressure was decreased to 800 psi and low force amplification ratios were chosen for analysis. This allows us to maneuver the extender within 2 Hz. Matrix R in equation 21 is chosen as the performance matrix in the Cartesian coordinate frame.

$$R^{-1} = \alpha = \begin{bmatrix} 5 & 0 \\ 0 & 7 \end{bmatrix} \quad \text{for all } \omega \in [0, 5 \text{ Hertz}] \quad (21)$$

The above performance specification has force amplifications of 7 times in the y-direction and 5 times in the x-direction. Figure 16 depicts the history of the extender position along the x direction, as a function of time in an experiment where the human operator maneuvers the extender irregularly (i.e., randomly). Figure 17 shows the experimental values of the human force, f_h, and the load force, f_e, in the x-direction. Figure 18 shows the FFT of $f_e/(f_h - f_h^*)$ along the x-direction where the load force f_e is more than $(f_h - f_h^*)$ by a factor of 5. It can be seen that this ratio is preserved only within the extender bandwidth. Figure 19 shows f_e versus $(f_h - f_h^*)$ along the x-direction where the slope of -5 represents the force amplification by a factor of 5. Figures 20 through 23 are similar to Figures 16 through 19, except that they have a force amplification of 7 in the y-direction. Figure 21 shows two graphs versus time, $(f_h - f_h^*)$ and f_e along the y-direction where the load force, f_e, is more than $(f_h - f_h^*)$ by a factor of 7. Figure 22 shows the FFT of

f_e /(f_h- f_h^*) along the y-direction where the amplification of 7 is preserved within the extender bandwidth. Figures 24 and 25 show the extender position, human force and extender force in the y-direction when α = -19 which violates the stability criteria in inequality 15.
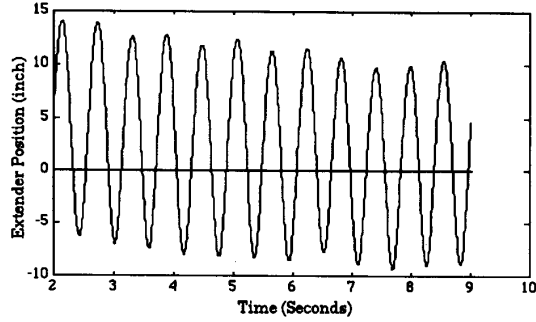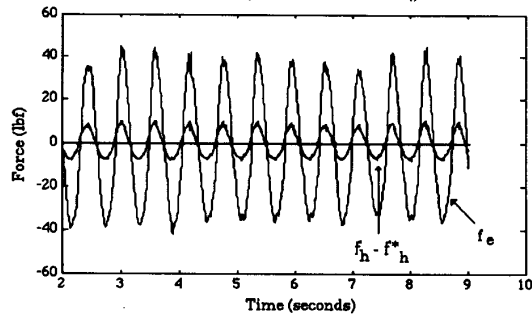

Figure 16: Extender position, x, shown in Figure 9.

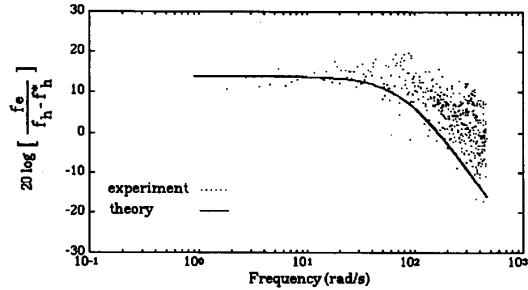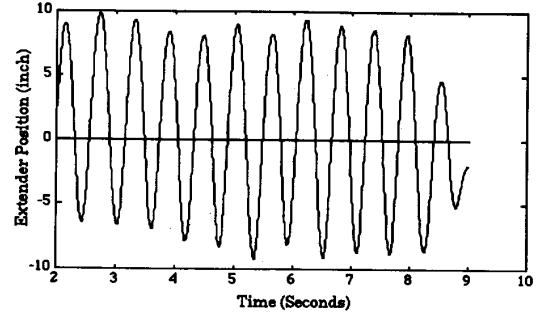Figure 17: Experimental human and load forces along the x direction. Force amplification ratio is 5.

Figure 18: Theoretical and experimental force amplification ratio along the x direction.
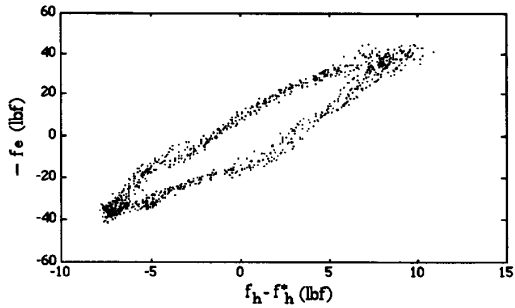
Figure 19: Load force versus human force along the x direction.Slope is approximately 5.

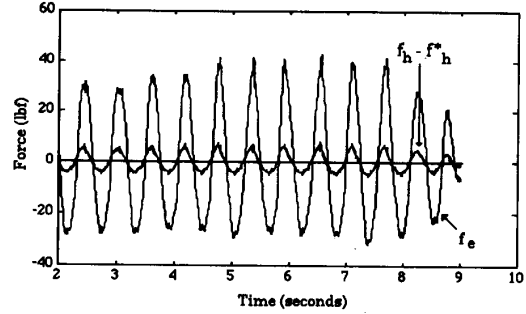
Figure 20: Extender position, y, measured from horizontal.

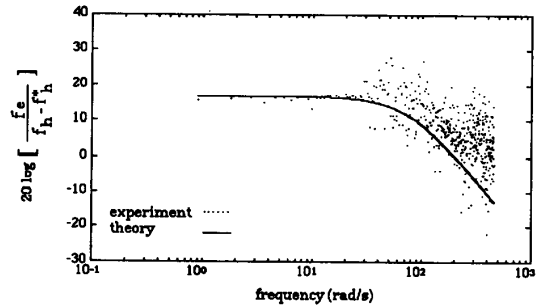Figure 21: Experimental human and load forces along the y direction. Force amplification ratio is 7.

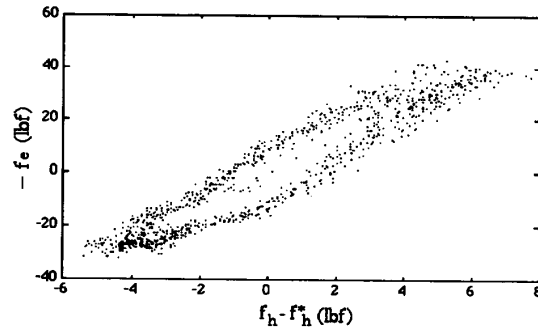Figure 22: Theoretical and experimental force amplification ratio along the y direction.

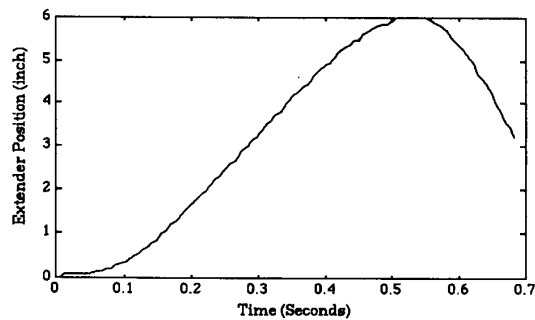Figure 23: Load force versus human force along the y direction. Slope is approximately 7.

— 19 —

Figure 24: Extender position, y, measured from horizontal, unstable maneuver.
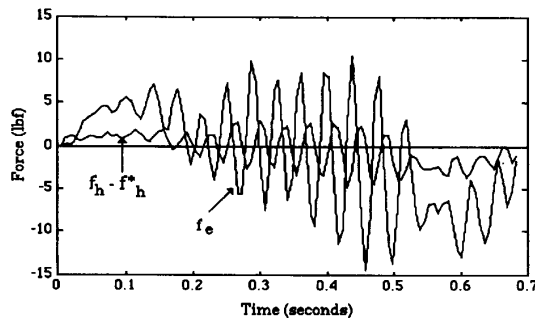

Figure 25: Experimental human and load forces. Force amplification ratio is 19.

7. SUMMARY AND CONCLUSION

This article describes the dynamics of human machine interaction in robotic systems worn by humans. These robots are referred to as extenders and amplify the strength of the human operator, while utilizing the intelligence of the operator to spontaneously generate the command signal to the system. Extenders augment human physical strength. System performance is defined as a linear relationship between the human force and the load force. A condition for stability of the total system (extender, human and the load) is derived, and, through experimentation, the performance is demonstrated. A six-degree-of-freedom extender has been built for experimental verification of the analysis.

8. REFERENCES

1. An, Chae H., Atkeson, Christopher G., Hollerbach, John M., "Model-Based Control of Robot Manipulator", MIT Press, 1988.
2. Asada, H., Slotine, J. E., "Robot Analysis and Control", Wiley, New York, 1986.
3. Berthoz, A., Metral, S., "Behavior of Muscular Group Subjected to a Sinusoidal and Trapezoidal Variation of Force", J. of Applied Physiol., Volume 29, pp:378-384, 1970.
4. Clark, D.C. et al., "Exploratory Investigation of the Man-Amplifier Concept", U.S. Air Force AMRL-TDR-62-89, AD-390070, August 1962.
5. Cooke, J. D., "Dependence of human arm movements in limb mechanical properties", Brain Res., Volume 165, pp: 366-369, 1979.
6. Cooke, J. D., "The Organization of Simple, Skilled Movements", Tutorials in Motor Behavior, edited by G. Stelmach and J. Requin, Amsterdam,: Elsevier, 1980.
7. Desoer, C. A., Vidyasagar, M., "Feedback Systems: Input-output Properties", Academic Press, 1975.
8. Feldman, A. G., "Functional tunning of the nervous system with control of movement or maintenance", J of Biophsics, V11, pp565-578.
9. GE Company, "Exoskeleton Prototype Project, Final Report on Phase I", Report S-67-1011, Schenectady, NY, 66.
10. GE Company, "Hardiman I Prototype Project, Special Interim Study", Report S-68-1060, Schnectady, NY, 1968.
11. Groshaw, P. F., "Hardiman I Arm Test, Hardiman I Prototype", Report S-70-1019, GE Company, Schenectady, NY, 1969.
12. Houk, J. C., "Neural control of muscle length and tension", in: Motor control, ed. V. B. Brooks. Bethesda, MD, American Physiological Society Handbook of Physiology.
13. Kazerooni, H., Waibel, B. J., "On the Stability of the Constrained Robotic Maneuvers in the Presence of Modeling Uncertainties," *IEEE Transaction on Robotics and Automation*, Vol. 7 No. 1. February 1991.
14. Kazerooni, H., "Human-Robot Interaction via the Transfer of Power and Information Signals", IEEE Transactions on Systems and Cybernetics, Vol. 20, No. 2, Mar. 1990.
15. Kazerooni, H., Mahoney, S., "Dynamics and Control of Robotic Systems Worn By Humans", ASME Journal of Dynamic Systems, Measurement, and Control. Vol. 133, No. 3. September 1991.
16. Kazerooni, H., Sheridan, T. B., and Houpt, P. K., "Fundamentals of Robust Compliant Motion for Manipulators," *IEEE Journal of Robotics and Automation*, Vol. 2, No. 2, June 1986.
17. Kazerooni, H., Waibel, B. J., and Kim, S., "Theory and Experiments on Robot Compliant Motion Control," *ASME Journal of Dynamic Systems Measurements and Control*, Vol. 112, No. 3, September 1990.
18. Kazerooni, H., "On the Contact Instability of the Robots When Constrained by Rigid Environments," *IEEE Transactions on Automatic Control*, Volume 35, Number 6, June 1990.
19. Marsden, C. D., Merton, P. A., Morton, H. B., " Stretch reflexes and servo actions in a variety of human muscles", Journal of Physiol., London, Volume 259, pp: 531-560.
20. Makinson, B. J., "Research and Development Prototype for Machine Augmentation of Human Strength and Endurance, Hardiman I Project", Report S-71-1056, General Electric Company, Schenectady, NY, 1971.
21. Merritt, H. E., "Hydraulic Control Systems", John Wiley & Sons, Inc., 1967.
22. Mizen, N. J., "Preliminary Design for the Shoulders and Arms of a Powered, Exoskeletal Structure", Cornell Aeronautical Laboratory Report VO-1692-V-4, 1965.
23. Mosher,R.S., "Force Reflecting Electrohydraulic Servomanipulator", Electro-Technology, pp. 138, Dec. 60.
24. Mosher, R. S., " Handyman to Hardiman", SAE Report 670088.
25. Repperger, D. W., Morris, A., "Discriminant Analysis of Changes in Human Muscle Function When Interacting with an Assistive Aid", IEEE Transaction on Biomedical Engineering, Vol. 35, No. 5, May 1988.
26. Sheridan, T. B., Ferrell, W. R., Man-Machine Systems: Information, Control, and Decision, Model of Human Performance, MIT Press, 1974.
27. Stein, R. B., "What muscles variables does the nervous system control in limb movements?", J. of the behavioral and brain sciences, 1982, Volume 5, pp 535-577.
28. Spong, M. W., Vidyasagar, M., "Robust Nonlinear Control of Robot Manipulators", Proc. 24th IEEE CDC, Ft. Lauderdale, FL, Dec. 1985.